Using Dedicated Time-Domain Basis Functions for the Simulation of Pulse-Width-Modulation Controlled Devices – Application to the Steady-State Regime of a Buck Converter

Johan Gyselinck [1], Claudia Martis [2] and Ruth V. Sabariego [3]

[1] Université Libre de Bruxelles (ULB), BEAMS dpt., Belgium
[2] Technical University of Cluj-Napoca, Electrical Machines and Drives dpt., Romania
[3] KU Leuven, Electrical Engineering dpt. (ESAT), Belgium

In this paper the authors present a novel approach for the time-stepping simulation of electrical devices with pulse-width-modulated (PWM) supply, based on so-called PWM basis functions which are periodic in time (at the switching frequency), piecewise polynomial and duty-cycle dependent. The state variables of the device's lumped-parameter circuit and/or finite element model are expanded in terms of these basis functions, with slowly varying coefficients in time. This allows for a large PWM-switching-frequency-independent time step and thus significant computational savings. By way of validation, the approach is applied to a buck converter in continuous-conduction mode. For this particular application, the steady-state waveforms of the inductor current and the output (capacitor) voltage are obtained through the resolution of a system of algebraic equations. As the set of the PWM basis functions is enlarged (with increasing polynomial degree), the respective PWM ripple components are observed to converge quickly to those obtained with plain time stepping (using a very small time step).

***Index Terms*— Circuit equations, time stepping, pulse width modulation, Galerkin method of weighted residuals, basis functions, buck converter, finite element modelling.**

I. Introduction

Pulse Width Modulation (PWM) is commonly used in power electronics for controlling various types of converters and applications (DC supplies, electrical drives, ...). The PWM switching of the supply quantity, e.g. the voltage or voltages in Voltage-Source Converters (VSCs), generates a ripple in all other quantities (currents, voltages, torque, ...). The amplitude of the ripple (at the switching frequency f_s) is kept small thanks to adequate passive filtering components (i.e. inductances and capacitors) and a sufficiently high switching frequency. The tendency is to further increase the latter given the technological progress in the domain of semiconductor power components and control electronics, allowing reducing converter cost and size [1].

The transient time-domain (time-stepping) analysis of these PWM converters and applications can be performed at three different levels, depending on 1) the purpose of the analysis, 2) the level of detail of the component models required and 3) the time-step size. When the detailed switching behaviour of the semiconductor components needs to be considered, e.g. for snubber design, sufficiently fine models of these components are required, combined with a very small time step to capture the switching transients. At an intermediate level, the semiconductor components are modelled in a very simple or idealised way, so that the application can be studied in more detail (e.g. using a finite element (FE) model), still with a time step which is much smaller than the switching period [2]. A further simplification consists in considering, e.g., the PWM voltage(s) at the input terminals of the application. The power electronic converter is thus not explicitly modelled, common practice for studying e.g. inverter-fed electrical machines and estimating the additional iron losses due to the PWM harmonics [3][4]. In the latter application, the switching instants are known *a priori*, what can be exploited for optimising the time-stepping scheme [4].

More flexible methods could be used to deal with the two time scales clearly present in PWM devices, i.e. the slow variation at the fundamental supply frequency or due to macroscopic transients versus the quick variation in the PWM ripple. Co-simulation of coupled field/circuit problems consists in using different and adapted time steps for each subproblem together with a more or less complicated synchronization [5].

The method presented in this paper is straightforwardly applicable in the particular case of *a priori* known PWM voltage, which implies that some parasitic effects of the converter are neglected (voltage drop across conducting power electronic switches and diodes, dead time, ...). The PWM ripple of the different state variables of the problem at hand is then approximated by so-called PWM basis functions (BFs). As the associated coefficients vary slowly in time, the resulting system of ordinary differential equations (ODEs) can be solved with a big switching-frequency-independent time step.

The method is applied to a simple test case, namely a buck converter in continuous-conduction mode [6]; the circuit and some results obtained by plain time stepping are presented in section II. In section III, the PWM-BFs are introduced. The new system of ODEs is derived in section IV by applying the standard Galerkin method to the time dimension. This is in fact an extension of the Harmonic Balance FE (HBFE) modelling of electromagnetic devices and rotating machines proposed in [7], [8]. In section V, results obtained for the steady-state DC regime of the buck converter are presented. When increasing the degree of the PWM-BFs (up to 8), excellent convergence towards to the waveforms obtained with plain time stepping (with a very small time step) is observed.

II. Test Case: Buck Converter

Figure 1 shows the well-known buck converter circuit, with DC voltage source at the input (constant DC voltage V_i assumed), a switch (an IGBT e.g.), a diode, an inductor (inductance L and resistance R_L), a capacitor (capacitance C), and a load resistance R connected to the output.

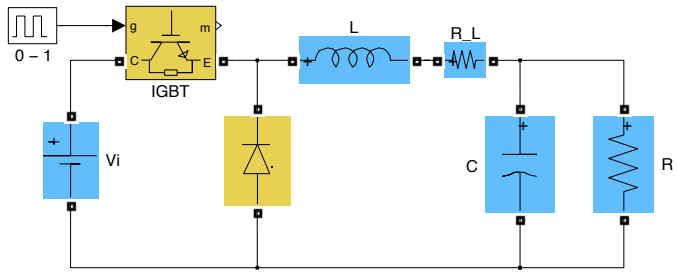

Fig. 1. Buck converter with DC voltage source, switch and diode (implementation in MATLAB/Simulink using the SimPowerSystems toolbox)

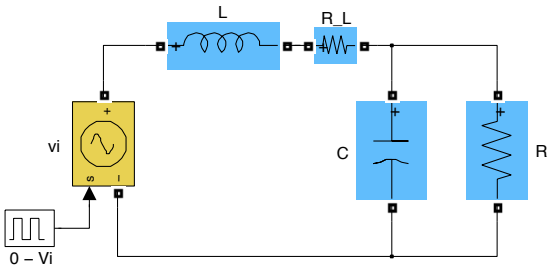

Fig. 2. Simplified buck converter circuit with PWM voltage at the input (continuous-conduction mode only)

The switch is closed and opened at switching frequency f_s (switching period $T_\mathrm{s} = 1/f_\mathrm{s}$), with duty cycle D ($0 \le D \le 1$).

Considering an ideal switch and an ideal diode (or a simple static model, as in the SimPowerSystems toolbox of MATLAB/Simulink), the circuit can be described by two state variables, namely the current through the inductor, $i_\mathrm{L}(t)$, and the voltage across the capacitor, $v_\mathrm{C}(t)$, the latter being the output voltage of the buck converter as well.

Assuming further continuous-conduction mode ($i_\mathrm{L} > 0$ at all times), the simplified circuit of Figure 2 can be considered. Herein the voltage source at the input produces a PWM voltage $v_\mathrm{i}(t)$, equal to either 0 or V_i. As the switch and diode are assumed ideal, we arrive at two first-order linear ODEs:

$$\begin{bmatrix} R_\mathrm{L} & 1 \\ -1 & 1/R \end{bmatrix} \begin{bmatrix} i_\mathrm{L} \\ v_\mathrm{C} \end{bmatrix} + \begin{bmatrix} L & 0 \\ 0 & C \end{bmatrix} \frac{\mathrm{d}}{\mathrm{d}t} \begin{bmatrix} i_\mathrm{L} \\ v_\mathrm{C} \end{bmatrix} = \begin{bmatrix} v_\mathrm{i}(t) \\ 0 \end{bmatrix}. \quad (1)$$

The following parameter values are adopted hereafter:

- $V_\mathrm{i} = 100\,\mathrm{V}$;
- $f_\mathrm{s} = 500\,\mathrm{Hz}$ or $5000\,\mathrm{Hz}$;
- $D = 0.7$;
- $L = 1\,\mathrm{mH}$, $R_\mathrm{L} = 10\,\mathrm{m\Omega}$;
- $C = 100\,\mu\mathrm{F}$;
- $R = 0.8\,\Omega$.

The plain time-stepping resolution of (1) is carried out with the ode23tb MATLAB solver. We start at $t = 0$ with zero initial current and voltage and go till $t = 25\,\mathrm{ms}$ for reaching steady-state regime with high accuracy (i.e. 12.5 and 125 PWM periods at 500 and 5000 Hz, respectively).

Figure 3 shows the PWM input voltage $v_\mathrm{i}(t)$, the voltage across the capacitor $v_\mathrm{C}(t)$ and the current in the inductor $i_\mathrm{L}(t)$ versus time with $f_\mathrm{s} = 500\,\mathrm{Hz}$. For obtaining a very accurate reference solution, the relative tolerance of the ode23tb solver is set to 10^{-6}. This results in 46320 variable-size time steps, or in average 3706 steps per PWM period.

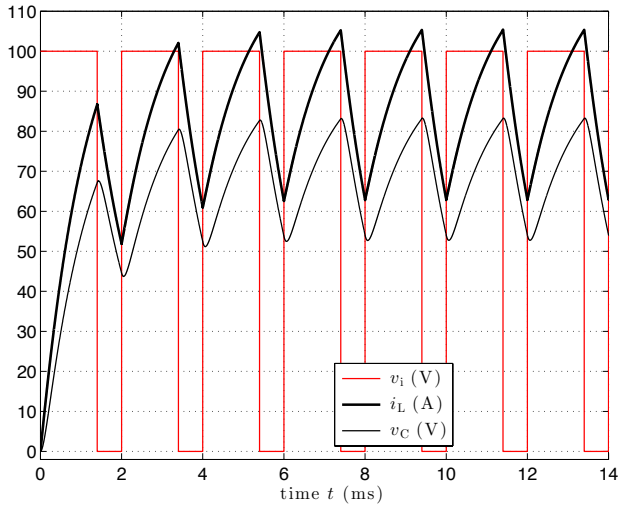

Fig. 3. PWM input voltage $v_\mathrm{i}(t)$, voltage across the capacitor $v_\mathrm{C}(t)$ and current in the inductor $i_\mathrm{L}(t)$ versus time with $f_\mathrm{s} = 500\,\mathrm{Hz}$

The result with $f_\mathrm{s} = 5000\,\mathrm{Hz}$ is depicted in Figure 4. The total number of time steps (same solver and tolerance) is 124472, or in average 996 steps per PWM period. The (peak-to-peak) current and voltage ripple is obviously much smaller than in the 500 Hz case, by roughly a factor 10 and 100, respectively.

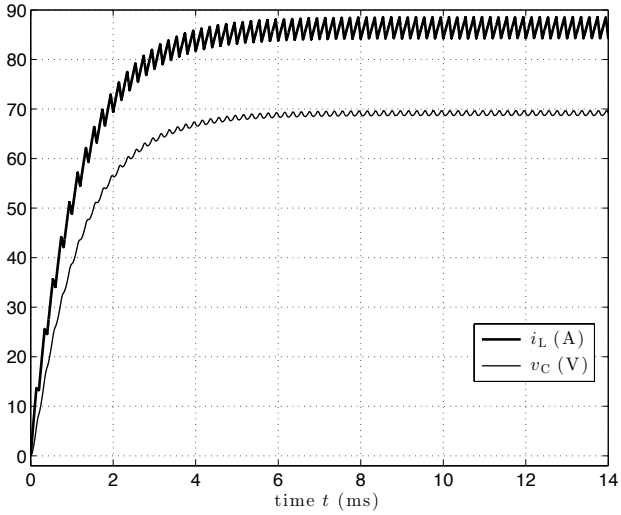

Fig. 4. Voltage across the capacitor $v_\mathrm{C}(t)$ and current in inductor $i_\mathrm{L}(t)$ versus time with $f_\mathrm{s} = 5000\,\mathrm{Hz}$

III. Orthonormal PWM basis functions

In the following the proposed method will be formally developed considering a general circuit governed by a system of N_s first-order linear ODEs:

$$\boldsymbol{A}\,\boldsymbol{X}(t) + \boldsymbol{B}\,\frac{\mathrm{d}\boldsymbol{X}}{\mathrm{d}t} = \boldsymbol{C}(t)\,, \tag{2}$$

where $\boldsymbol{X}$ is the vector ($N_\mathrm{s} \times 1$ matrix) of state variables

$$\boldsymbol{X}(t) = \begin{bmatrix} x_1(t) \\ x_2(t) \\ \vdots \\ x_{N_\mathrm{s}}(t) \end{bmatrix}, \tag{3}$$

$\boldsymbol{A}$ and $\boldsymbol{B}$ are constant $N_\mathrm{s} \times N_\mathrm{s}$ matrices, and $\boldsymbol{C}(t)$ is a $N_\mathrm{s} \times 1$ matrix which depends on the PWM voltages (with parameters f_s and D).

All state variables are further assumed continuous (with generally discontinuous time derivative as a result of the switching); this determines the choice of the BFs.

Throughout this paper matrices are denoted by bold upper-case letters. For those related to the PWM-BFs, introduced below, bold calligraphic uppercase letters are adopted, namely $\boldsymbol{\mathcal{P}}$, $\boldsymbol{\mathcal{X}}_j$, $\boldsymbol{\mathcal{X}}$, $\boldsymbol{\mathcal{Q}}$, $\boldsymbol{\mathcal{A}}$, $\boldsymbol{\mathcal{B}}$, $\boldsymbol{\mathcal{C}}$.

Each state variable $x_j(t)$, $0 \le j \le N_\mathrm{s}$, is expanded in terms of $N_\mathrm{p}+1$ periodic BFs $p_k(t)$, $0 \le k \le N_\mathrm{p}$, and associated coefficients $x_{j,k}(t)$:

$$x_j(t) = \sum_{k=0}^{N_\mathrm{p}} p_k(t)\, x_{j,k}(t)\,. \tag{4}$$

The periodicity with period $T_\mathrm{s} = 1/f_\mathrm{s}$, i.e. $p_k(t+T_\mathrm{s}) = p_k(t)$, is easily accounted for by introducing the relative time τ ($0 \le \tau \le 1$):

$$\tau \;=\; \frac{t}{T_\mathrm{s}} \text{ modulo } 1\,. \tag{5}$$

It is further assumed that the switching (closing/opening of the switch) occurs at $\tau = 0$ (or $\tau = 1$) and $\tau = D$ respectively.

The BFs p_k will from here on be expressed in terms of $\tau(t)$. Their periodicity then reads:

$$p_k(1) = p_k(0)\,. \tag{6}$$

The first BF ($k = 0$) is constant and allows to capture the slow variation of the state variables (coefficients $x_{j,0}$):

$$p_0 = 1\,. \tag{7}$$

The terms in (4) with $k > 0$ constitute the PWM ripple referred to as $\tilde{x}_j$:

$$\tilde{x}_j(t) = \sum_{k=1}^{N_\mathrm{p}} p_k(t)\, x_{j,k}(t)\,. \tag{8}$$

The BFs $p_k(\tau)$ used for approximating the PWM ripple, with $1 \le k \le N_\mathrm{p}$, are piecewise polynomial (of degree k) in the two respective intervals $]0, D[$ en $]D, 1[$. The complete set of $N_\mathrm{p}+1$ BFs $p_k(\tau)$ is further orthonormalised,

$$\int_0^1 p_k(\tau)\, p_l(\tau)\, \mathrm{d}\tau = \begin{cases} 1 & \text{if } k = l \\ 0 & \text{if } k \ne l \end{cases} \tag{9}$$

as detailed below.

The piecewise linear BF $p_1(\tau)$ defined as:

$$p_1(\tau) \;=\; \begin{cases} \sqrt{3}\,\frac{2\tau - D}{D} & \text{if} \quad 0 \le \tau \le D \\ \sqrt{3}\,\frac{1+D-2\tau}{1-D} & \text{if} \quad D \le \tau \le 1 \end{cases} \tag{10}$$

varies between $-\sqrt{3}$ (at τ equal to 0 and 1) and $\sqrt{3}$ (at $\tau = D$), has zero average value and is normalised.

The BFs $p_k(\tau)$, $2 \le k \le N_\mathrm{p}$, are obtained recursively by integrating $p_{k-1}(\tau)$:

$$p_k^\star(\tau) = \int_0^\tau p_{k-1}(\tau')\, \mathrm{d}\tau'\,, \tag{11}$$

thus ensuring C0 continuity, and next orthonormalising the extended set of BFs by means of $k+1$ factors n_k and $o_{k,l}$:

$$p_k(\tau) = n_k\, p_k^\star(\tau) + \sum_{l=0}^{k-1} o_{k,l}\, p_l(\tau)\,. \tag{12}$$

The thus defined orthonormal PWM-BFs $p_0(\tau)$ till $p_8(\tau)$ are shown in Figure 5. Note that the PWM-BFs $p_k(\tau)$ depend on the duty cycle D but not on the switching frequency f_s.

From (4) the time derivative of $x_j(t)$ is given by:

$$\frac{\mathrm{d}x_j}{\mathrm{d}t} \;=\; \sum_{k=0}^{N_\mathrm{p}} \left(\frac{\mathrm{d}p_k}{\mathrm{d}\tau}\,\frac{\mathrm{d}\tau}{\mathrm{d}t}\, x_{j,k}(t) + p_k(t)\,\frac{\mathrm{d}x_{j,k}}{\mathrm{d}t} \right), \tag{13}$$

with

$$\frac{\mathrm{d}\tau}{\mathrm{d}t} = \frac{1}{T_\mathrm{s}} = f_\mathrm{s}\,. \tag{14}$$

The expansion of state variable $x_j(t)$ in terms of the $N_\mathrm{p}+1$ basis functions $p_k(\tau)$ is written in matrix form as:

$$x_j(t) = \boldsymbol{\mathcal{P}}^\top(\tau(t))\, \boldsymbol{\mathcal{X}}_j(t)\,, \tag{15}$$

where the $(N_\mathrm{p}+1) \times 1$ matrices $\boldsymbol{\mathcal{P}}(\tau)$ and $\boldsymbol{\mathcal{X}}_j(t)$ are given by

$$\boldsymbol{\mathcal{P}}(\tau) = \begin{bmatrix} p_0 \\ p_1(\tau) \\ p_2(\tau) \\ \vdots \\ p_{N_\mathrm{p}}(\tau) \end{bmatrix}, \qquad \boldsymbol{\mathcal{X}}_j \;=\; \begin{bmatrix} x_{j,0}(t) \\ x_{j,1}(t) \\ x_{j,2}(t) \\ \vdots \\ x_{j,N_\mathrm{p}}(t) \end{bmatrix}, \tag{16}$$

with, as a reminder, $p_0 = 1$.

The time derivative of $x_j(t)$ reads:

$$\frac{\mathrm{d}x_j}{\mathrm{d}t} \;=\; f_\mathrm{s}\,\frac{\mathrm{d}\boldsymbol{\mathcal{P}}^\top}{\mathrm{d}\tau}\,\boldsymbol{\mathcal{X}}_j(t) + \boldsymbol{\mathcal{P}}^\top(\tau)\,\frac{\mathrm{d}\boldsymbol{\mathcal{X}}_j}{\mathrm{d}t}\,. \tag{17}$$

Note that in case of steady-state DC regime (at constant duty cycle D), all $\boldsymbol{\mathcal{X}}_j$'s are constant and the second term in the right-hand side of (17) cancels.

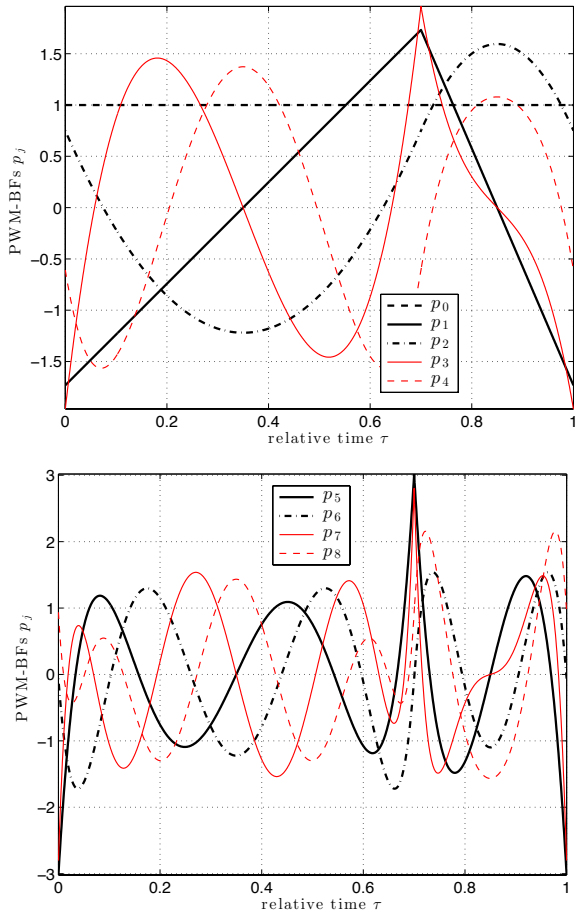

Fig. 5. PWM-BFs $p_0(\tau)$ to $p_8(\tau)$ for $D = 0.7$

In matrix form the orthonormality of the PWM-BFs can be expressed as

$$\int_0^1 \boldsymbol{\mathcal{P}}(\tau)\,\boldsymbol{\mathcal{P}}^\top(\tau)\,\mathrm{d}\tau \;=\; \boldsymbol{I}\,, \tag{18}$$

where $\boldsymbol{I}$ is the $(N_\mathrm{p}+1)\times(N_\mathrm{p}+1)$ identity matrix.

Let us further introduce the following matrix:

$$\boldsymbol{\mathcal{Q}} \;=\; \int_0^1 \boldsymbol{\mathcal{P}}(\tau)\,\frac{\mathrm{d}\boldsymbol{\mathcal{P}}^\top}{\mathrm{d}\tau}\,\mathrm{d}\tau\,. \tag{19}$$

IV. Steady-state equations with PWM-BFs

Writing the N_s state variables $x_j(t)$ in terms of the $N_\mathrm{p}+1$ PWM-BFs $p_{j,k}(\tau)$:

$$\boldsymbol{X}(t) = \begin{bmatrix} x_1(t) \\ x_2(t) \\ \vdots \end{bmatrix} = \begin{bmatrix} \boldsymbol{\mathcal{P}}(\tau)\boldsymbol{\mathcal{X}}_1(t) \\ \boldsymbol{\mathcal{P}}(\tau)\boldsymbol{\mathcal{X}}_2(t) \\ \vdots \end{bmatrix}, \tag{20}$$

a total of $N_\mathrm{sp} = N_\mathrm{s}(N_\mathrm{p}+1)$ state variables $x_{j,k}(t)$ results.

The latter vary slowly though, allowing a big time step. In case of steady-state DC regime, as focused on in this paper for the buck converter, the state variables $x_{j,k}$ are even constant (and are to be obtained by solving a system of algebraic equations).

The original system of N_s ODEs (2) is weakly enforced by weighing them with each of the $N_\mathrm{p}+1$ PMW-BFs $p_l(\tau)$ in an interval $[t - T_\mathrm{s}/2, t + T_\mathrm{s}/2]$:

$$\int_{t-T_\mathrm{s}/2}^{t+T_\mathrm{s}/2} \left(\boldsymbol{A}\,\boldsymbol{X}(t) + \boldsymbol{B}\,\frac{\mathrm{d}\boldsymbol{X}}{\mathrm{d}t} - \boldsymbol{C}(t)\right) p_l(\tau(t))\,\mathrm{d}t \;=\; 0\,, \tag{21}$$

i.e. Galerkin's method applied to the time dimension [7], [8].

Assembling all N_sp variables

$$\boldsymbol{\mathcal{X}}(t) = \begin{bmatrix} \boldsymbol{\mathcal{X}}_1(t) \\ \boldsymbol{\mathcal{X}}_2(t) \\ \vdots \end{bmatrix}, \tag{22}$$

the system of N_sp ODEs from (21) can be written as

$$\boldsymbol{\mathcal{A}}\,\boldsymbol{\mathcal{X}}(t) + \boldsymbol{\mathcal{B}}\,\frac{\mathrm{d}\boldsymbol{\mathcal{X}}}{\mathrm{d}t} \;=\; \boldsymbol{\mathcal{C}}(t)\,, \tag{23}$$

with

$$\boldsymbol{\mathcal{A}} = \begin{bmatrix} A_{11}\boldsymbol{I} & A_{12}\boldsymbol{I} & \dots \\ A_{21}\boldsymbol{I} & A_{22}\boldsymbol{I} & \dots \\ \vdots & \vdots & \ddots \end{bmatrix} + f_\mathrm{s} \begin{bmatrix} B_{11}\boldsymbol{\mathcal{Q}} & B_{12}\boldsymbol{\mathcal{Q}} & \dots \\ B_{21}\boldsymbol{\mathcal{Q}} & B_{22}\boldsymbol{\mathcal{Q}} & \dots \\ \vdots & \vdots & \ddots \end{bmatrix}, \tag{24}$$

$$\boldsymbol{\mathcal{B}} = \begin{bmatrix} B_{11}\,\boldsymbol{I} & B_{12}\,\boldsymbol{I} & \dots \\ B_{21}\,\boldsymbol{I} & B_{22}\,\boldsymbol{I} & \dots \\ \vdots & \vdots & \ddots \end{bmatrix}, \tag{25}$$

$$\boldsymbol{\mathcal{C}}(t) = \int_{t-T_\mathrm{s}/2}^{t+T_\mathrm{s}/2} \begin{bmatrix} C_1(t)\,\boldsymbol{\mathcal{P}}(\tau(t)) \\ C_2(t)\,\boldsymbol{\mathcal{P}}(\tau(t)) \\ \vdots \end{bmatrix} \mathrm{d}t\,. \tag{26}$$

Note that the $N_\mathrm{sp}\times N_\mathrm{sp}$ matrix $\boldsymbol{\mathcal{B}}$ is independent of the switching frequency f_s, whereas $\boldsymbol{\mathcal{A}}$ depends on f_s as it appears explicitly in (24). The $N_\mathrm{sp}\times 1$ matrix $\boldsymbol{\mathcal{C}}(t)$ depends on the PWM source voltage ($C_1(t) = v_\mathrm{i}$ and $C_2 = 0$ in case of the buck converter).

In steady-state DC regime, $\boldsymbol{\mathcal{X}}$ is constant and a system of N_sp algebraic equations results:

$$\boldsymbol{\mathcal{A}}\,\boldsymbol{\mathcal{X}} = \boldsymbol{\mathcal{C}}\,. \tag{27}$$

V. Application to test case

We now apply the above presented PWM-BF approach to the buck converter case described by the system of ODEs (1), with the parameter values listed above and f_s equal to either 500 Hz or 5000 Hz. For each frequency, a very precise reference solution is obtained (as detailed in section II), from which a reference steady-state solution, denoted by $x_{j,\mathrm{ref}}(\tau)$, is extracted (with $x_1 = i_\mathrm{L}$ and $x_2 = v_\mathrm{C}$); subtraction of the respective average values gives the PWM ripple component denoted by $\tilde{x}_{j,\mathrm{ref}}(\tau)$. For the error analysis, the rms value of the ripple component is considered:

$$\tilde{x}_{j,\mathrm{ref,rms}} \;=\; \sqrt{\int_0^1 \tilde{x}^2_{j,\mathrm{ref}}(\tau)\,\mathrm{d}\tau}\,. \tag{28}$$

As for the PWM-BF approach, N_p is successively increased from 1 up to 8, each case requiring the solution of a system

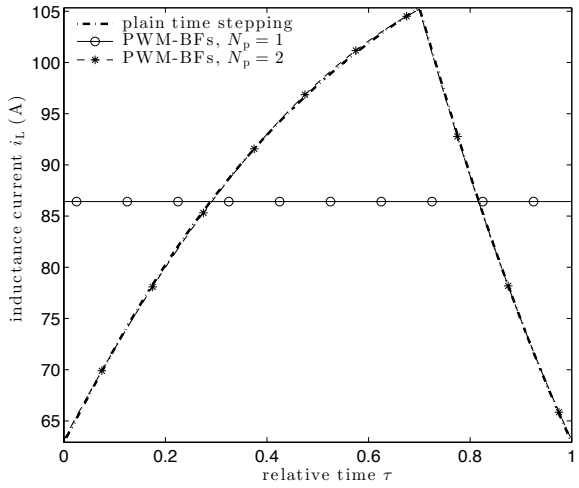

Fig. 6. Steady-state $i_{\mathrm{L}}(\tau)$ at 500 Hz

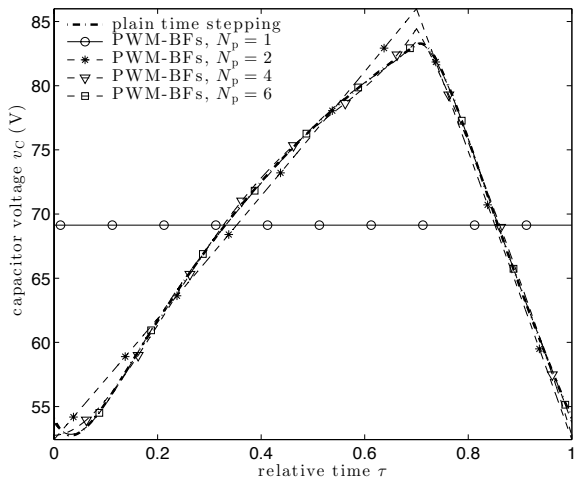

Fig. 7. Steady-state $v_{\mathrm{C}}(\tau)$ at 500 Hz

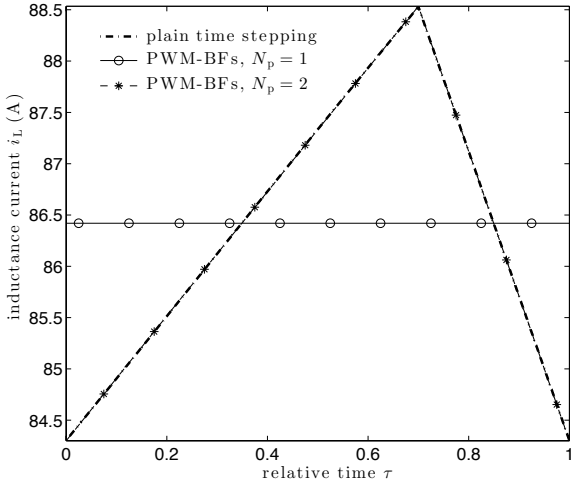

Fig. 8. Steady-state $i_{\mathrm{L}}(\tau)$ at 5000 Hz

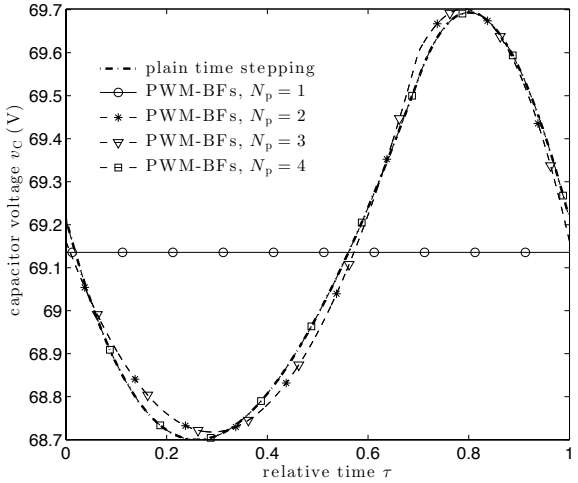

Fig. 9. Steady-state $v_{\mathrm{C}}(\tau)$ at 5000 Hz

of N_{sp}, i.e. 4 up to 18, algebraic equations. The PWM-BF solution is denoted by $x_{j,N_{\mathrm{p}}}$, and its ripple component by $\tilde{x}_{j,N_{\mathrm{p}}}$.

The relative rms value of the error of the ripple component of the PWM-BF solution is taken as global measure of accuracy of the proposed approach:

$$\varepsilon_{j,N_{\mathrm{p}}} = \frac{\sqrt{\int_0^1 \left(\tilde{x}_{j,\mathrm{ref}} - \tilde{x}_{j,N_{\mathrm{p}}}\right)^2 \mathrm{d}\tau}}{\tilde{x}_{j,\mathrm{ref,rms}}} \,. \tag{29}$$

Its value depends on the switching frequency f_{s}, the state variable (index j) and the degree N_{p} of the PWM-BF expansion, all other parameters kept constant.

The reference steady-state waveforms $i_{\mathrm{L,ref}}(\tau)$ and $v_{C,\mathrm{ref}}(\tau)$ are shown in Figures 6 and 7 for $f_{\mathrm{s}} = 500\,\mathrm{Hz}$, together with PWM-BF solutions $i_{\mathrm{L},N_{\mathrm{p}}}(\tau)$ and $v_{\mathrm{C},N_{\mathrm{p}}}(\tau)$. The PWM-BF approach with $N_{\mathrm{p}} = 1$ produces only the average value of i_{L} and v_{C}; with $N_{\mathrm{p}} = 2$ the waveform of i_{L} is already quite close to the reference one, whereas for v_{C}, N_{p} should be increased further for getting a similar accuracy.

The steady-state waveforms with $f_{\mathrm{s}} = 5000\,\mathrm{Hz}$ are depicted in Figures 8 and 9. They are apparently closer to the ones of the classical simplified theoretical analysis, i.e. piecewise linear for i_{L} and piecewise parabolic for v_{C} [6]. As a consequence, the solution obtained with the PWM-BFs converges more quickly with increasing N_{p}.

The excellent convergence of the PWM-BF solution observed in Figures 6-9 is confirmed by the error curves shown in Figures 10 and 11. In the latter figure, the (implementation-dependent) round-off error becomes apparently preponderant from $N_{\mathrm{p}} = 6$ on.

VI. Conclusion

The concept of the PWM-BF approach has been convincingly proved by means of a simple linear test case with one constant duty cycle and looking at the steady-state DC regime. The application scope can be straightforwardly extended, considering next transient operation, a saturable inductor and one or more variable (sinusoidal) duty cycles.

References

[1] B.K. Bose, "Power electronics and motor drives: advances and trends." Academic Press, 2006. Access online via Elsevier.

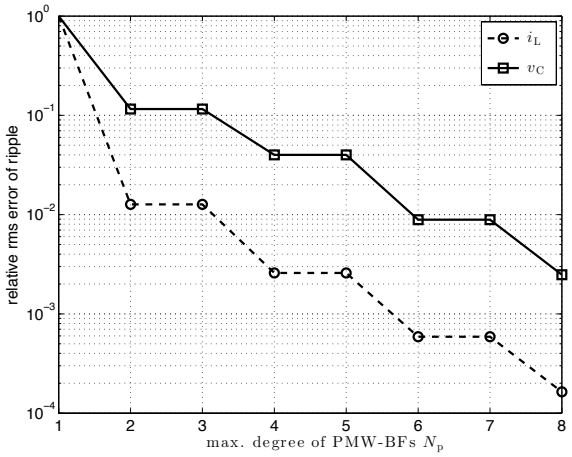

Fig. 10. Relative rms error of $\tilde{i}_\mathrm{L}$ and $\tilde{v}_\mathrm{C}$ as a function of N_p with $f_\mathrm{s} = 500\,\mathrm{Hz}$

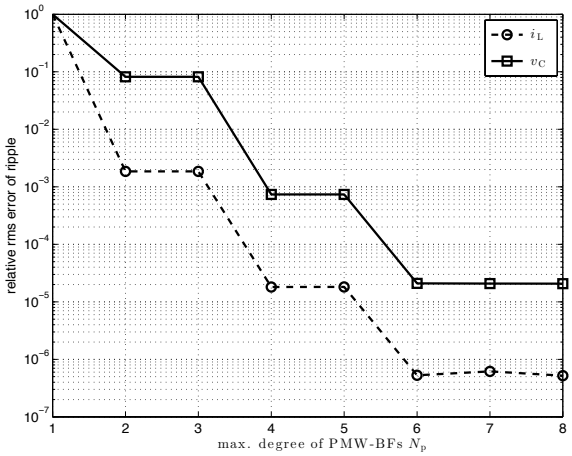

Fig. 11. Relative rms error of $\tilde{i}_\mathrm{L}$ and $\tilde{v}_\mathrm{C}$ as a function of N_p with $f_\mathrm{s} = 5000\,\mathrm{Hz}$

[2] M. van der Giet, E. Lange, D. Correa, I. Chabu, S. Nabeta, K. Hameyer (2010). "Acoustic simulation of a special switched reluctance drive by means of fieldcircuit coupling and multiphysics simulation," *IEEE Trans. on Industrial Electronics*, vol. 57, pp. 2946–2953, 2010.

[3] P. Rasilo, A. Arkkio, "Modeling the effect of inverter supply on eddy-current losses in synchronous machines," Proceedings SPEEDAM 2010.

[4] A. Knight, J.C. Salmon, J. Ewanchuk, "Integration of a first order eddy current approximation with 2D FEA for prediction of PWM harmonic losses in electrical machines," *IEEE Trans. on Magn.*, vol. 49, pp. 1957–1960, 2013.

[5] S. Schops, H. De Gersem, A. Bartel, "Higher-order cosimulation of field/circuit coupled problems," *IEEE Trans. on Magn.*, vol. 48, pp. 535–538, 2012.

[6] N. Mohan, T.M. Undeland, "Power electronics: converters, applications, and design." Wiley India Pvt. Limited, 2007.

[7] J. Gyselinck, P. Dular, C. Geuzaine, W. Legros, "Harmonic-balance finite-element modeling of electromagnetic devices: a novel approach," *IEEE Trans. on Magn.*, vol. 38, pp. 521–524, 2002.

[8] J. Gyselinck, L. Vandevelde, P. Dular, C. Geuzaine, W. Legros, "A general method for the frequency domain FE modeling of rotating electromagnetic devices," *IEEE Trans. on Magn.*, vol. 39, pp. 1147–1150, 2003.